Theor Chem Account (2007) 118:807–812
DOI 10.1007/s00214-007-0324-4

REGULAR ARTICLE

A comparison between the absorption properties of the regular and F_s-defected MgO (100) surface

Giovanni Barcaro · Mauro Causà · Alessandro Fortunelli

Received: 30 January 2007 / Accepted: 25 April 2007 / Published online: 1 June 2007

Abstract The electron density, the electrostatic potential and the electric field of the MgO (100) surface, both regular and containing an oxygen vacancy (F_s center), are compared in order to understand the modifications induced in the surface-absorbate interaction by the presence of the defect, with particular attention to the metal-oxide case. The spin-density for a gold atom absorbing on the most characteristic sites of the regular and F_s-defected surface is also shown. It is found that in the defected surface the electron pair in the vacancy protrudes appreciably out of the surface, thus shifting the electrostatic potential to negative values (but producing a similar electric field) and being able to chemically interact with neighboring absorbed species. These results rationalize the rotational invariance and double frustration effects previously described for the metal/F_s-defected MgO (100) surface.

Keywords Oxide surfaces · Surface defects · Metal-on-oxide · Electrostatic potential · Electrostatic field

1 Introduction

Oxide surfaces are important for many scientific and technological applications, ranging from catalysis to chemical sensing, to their use as templates for the epitaxial growth of other oxides or for the deposition of nanosized metal clusters and other absorbates, etc. [1–8]. In this context, the MgO(100) surface has been intensively studied [9–13] for its technological (e.g., catalytic) applications, and for its potentialities as a support which is at the same time inert and able to modulate the absorbate charge distribution. Moreover, its theoretical description is simplified by the fact that this surface does not present the complications associated with surface reconstruction, MgO being a simple ionic solid and the MgO (100) surface being a non-polar one. Attention has been focused both on the regular surface, as it has been shown that MgO(100) films and single crystals of good quality can be prepared through various experimental protocols [12–14], and also on variously defected surfaces [9,15–17], with the goal of understanding the modifications induced by the defects on the adsorption properties of the oxide. Surface defectivity is particularly interesting in the case of MgO(100), as the defects can act as strong trapping (and thus nucleation) centers for the growth of absorbates: the same inert characteristics of this surface make that the absorbate growth is strongly influenced by the presence of defects. Among the possible surface defects, the neutral oxygen vacancy (also known as F_s center) has been intensively studied [18–30]: statical and dynamical properties, electron density, Bader and ELF maps, density of states plots, optical properties, etc. It has been shown that this defect is at the same time common on properly engineered surfaces [41] and able to act as a nucleation center for several species, such as for example gold clusters [19,31–33]. The strength of the Au atom/F_s-center bond in fact is estimated to be greater than 2.5 eV, thus providing a site at which nucleation can occur, as definitively confirmed by a recent combined EPR and theoretical characterization of a single gold atom interacting with the regular and defected MgO (100) surface [17]. In a previous work [35], we have performed systematic density-functional (DF) calculations focusing on the study of the interaction of small Au clusters with a neutral oxygen vacancy defect

G. Barcaro · A. Fortunelli (✉)
Molecular Modeling Laboratory, IPCF-CNR, Via G. Moruzzi 1, Pisa 56124, Italy
e-mail: fortunelli@ipcf.cnr.it

M. Causà
Università di Napoli "Federico II", Via Cintia, Napoli 80126, Italy

lying on a MgO(100) terrace. We have found that this defect induces a long-range modification of the metal absorption characteristics in its surrounding, and that this perturbation is responsible for the fluxionality of small clusters growing around the vacancy, possibly connected with the formation of clusters exhibiting different structural motifs. In the present work, we investigate in more detail the nature of the oxygen vacancy defect by comparing electron densities, electrostatic potentials and electric fields in presence and in absence of the defect, and the modifications the oxygen vacancy introduces in the absorbate/surface interaction, focusing attention on the absorption of a single gold atom as a prototypical case. This is achieved by decomposing the interaction energy in terms of repulsion, chemical bonding, electrostatic and polarization contribution, which allows us to show that the long-range enhancement in the absorbate/surface interaction induced by the F_s defect is due both to a chemical bonding effect and to an electrostatic effect.

2 Materials and methods

Density-functional (DF) calculations are performed using the CRYSTAL03 computational code [36]. The B3PW91 exchange-correlation functional [37], which is a hybrid functional, is used. A Gaussian-type-orbital basis set of double-zeta quality is used on both Mg and O. The contraction scheme (8-511G and 8-411G) is taken from refs. [38,40], and has been specifically derived for bulk MgO. This basis set can be found in the database of the CRYSTAL03 code (http://www.crystal.unito.it). In agreement with refs [38,40], we also found that such a basis set is able to produce a reasonable description of the MgO system and its electrostatic properties, even in the absence of polarization functions. The regular MgO (100) surface is modeled by a three layer-slab (as it is customary [23]), each containing 18 (3×3 cell) Mg and O atoms fixed at the equilibrium lattice positions characterizing the MgO rock-salt structure (frozen at the experimental lattice constant of 4.208 Å). To produce an F_s defected surface, we remove a neutral oxygen atom from a surface layer, keeping the positions of all the other atoms in the cell fixed.

All the pictures have been obtained by using the XCrySDen program [40].

3 Results

In the case of metal/defected-surface interaction, it has been previously shown [22,27,35] that the presence of an F_s center on the MgO (100) surface remarkably affects not only the interaction of the metal atoms on-top of the vacancy, but also the metal interaction with the surrounding surface sites in a region which extends up to 6–8 Å from the F_s center. For example, the absorption energy landscape of a single gold atom changes substantially when passing from the regular to the F_s-defected (100) surface. On the regular surface, one finds a rather flat potential energy surface, exhibiting minima on the oxygen atoms, maxima on the magnesium atoms, and saddle points on the hollow sites, with a maximum adhesion energy of 0.91 eV and energy barriers of about 0.2 eV for the diffusion between neighboring oxygen sites. Correspondingly, the equilibrium height exhibits minima at 2.30 Å on the oxygen sites, maxima at 2.71 Å on the magnesium sites, and saddle points at 2.40 Å on the hollow sites. The in-plane distance between the energy minima corresponds to the MgO lattice parameter of about 2.97 Å: this value is larger than the typical Au–Au distances (the Au–Au distance in the bulk is 2.885 Å; smaller distances are normally found in Au nanoclusters), thus inducing a frustration (mismatch) in the metal growth on the MgO (100) surface. The presence of the F_s defect completely alters this situation, with the resulting potential energy and equilibrium height surfaces exhibiting three major features: (i) the energy minimum in correspondance with the defect site is much deeper, with an adhesion energy of 3.07 eV; (ii) a large basin of attraction is produced around the defect, with an adhesion energy of 1.62 eV on the magnesium atoms first-neighbors to the vacancy (to be compared to a value of 0.5 eV for the regular surface), extending its influence up to third neighbors, and exhibiting an approximate *cylindrical symmetry*; (iii) there is a large difference between the equilibrium distance atop the defect (about 1.8 Å), strongly reduced with respect to the absorption onto the regular surface, and that atop the neighboring sites (2.65 and 2.59 Å on the magnesium and oxygen sites next to the defect, respectively), for which an increase in the absorption energy does not always correspond to a decrease of the equilibrium distances. This strong variation of $r_{\min}$ around the defect site entails that the growth of metal clusters is frustrated not only "horizontally" with respect to the surface, but also "vertically", due to the appreciable difference in the equilibrium height for the atom interacting directly with the F_s center and the neighboring atoms interacting with the surrounding sites, a feature which can be described as a *double frustration*.

In order to rationalize these features, we have performed a detailed analysis of the electronic density, the electrostatic potential and the electric field of the oxide in the case of the regular and of the F_s-defected MgO (100) surface.

We start with the analysis of the electron density. In Fig. 1 the HOMO orbital of the F_s-defected MgO (100) surface is displayed: this plot is obtained by performing a calculation at the Γ point of the Brillouin zone. The shape of this orbital, which lies in the band gap of the insulator oxide and presents a strong *s*-character, shows how the two electrons trapped in the cavity are not fully confined by the Madelung potential of

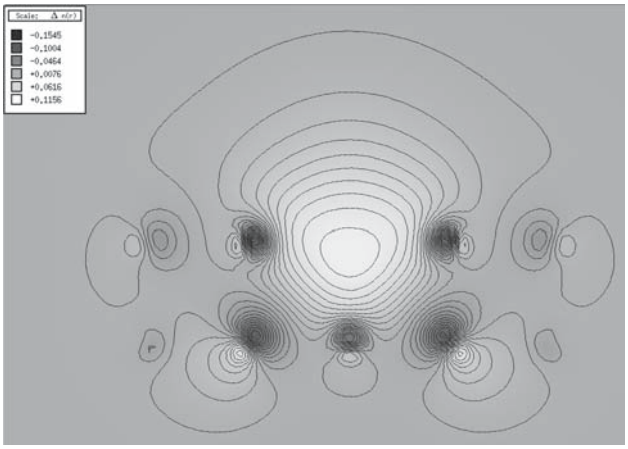

Fig. 1 Electron density contour of the HOMO orbital of the F_s defected MgO (100) surface: the two electrons in the vacancy are not well trapped by the Madelung potential and their density protrudes out of the cavity

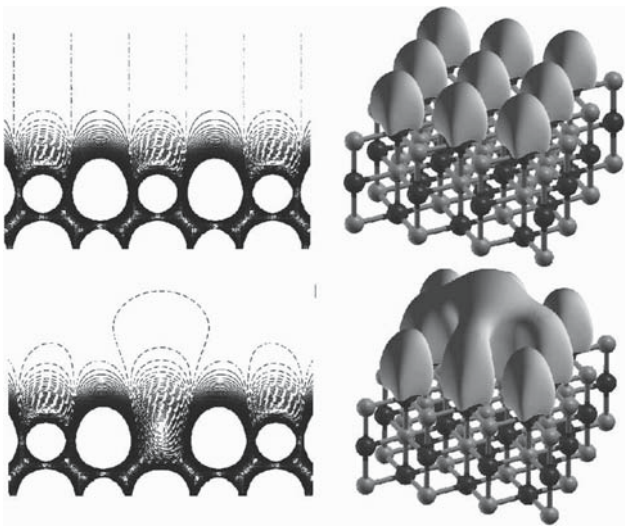

Fig. 2 Two dimensional and 3-D maps of the electrostatic potential generated by the regular (*first row*) and F_s-defected (*second row*) MgO (100) surface; in the 3-D maps, isosurfaces of value −0.0005 a.u. are shown

the solid; their density, on the contrary, protrudes out of the cavity and extends also above the sites around the vacancy [19,21,22].

This charge delocalization produces different patterns of electrostatic potential in the presence of the defect with respect to the regular surface. As can be observed in Fig. 2, in fact, in the case of the regular surface the absolute value of the electrostatic potential is almost the same on the oxygen and on the magnesium sites. This is due to the fact that, at a good approximation, this solid is ionic, with the same amount of positive and negative charge on the oxygen and magnesium sites. On the contrary, when the oxygen atom is missing and the negative charge protrudes out of the vacancy, an enhanced negative potential, which extends also to the neighbor sites around the defect, is observed.

To give a more quantitative estimate of this phenomenon, Fig. 3 illustrates the behavior of the electrostatic potential along the direction perpendicular to the (100) terrace and atop different sites of the regular and defected surfaces. Figure 3a refers to the regular surface: the dashed line shows the potential atop the magnesium site, whereas the continuous line shows the potential atop the oxygen site; as discussed above, the two behaviors are similar in absolute value, and opposite in sign. Figure 3b refers to the F_s-defected surface; the dashed line shows the potential directly atop the defect: this curve is strongly shifted towards negative values, because of the delocalization of the two electrons in the cavity. Since this delocalization implies spreading over the neighboring sites, also the other curves are negatively shifted: moreover, as the magnesium site is closer to the defect, the corresponding potential curve (dashed line) is more negatively shifted than the curve relating to the oxygen site first neighbor to the vacancy (continuous line) for distances greater than 3.7 Å. Finally, a further effect of the charge spreading out of the cavity is that all the potential curves go to zero much more slowly, and not monotonously, than in the case of regular surface.

When a metal atom is absorbed atop the defect, the remarkable increase of its interaction energy (which amounts, in the case of gold, to 3.07 eV instead of 0.91 eV) can be decomposed into three contributions: (i) The absence of the oxygen under the metal species determines a decrease of the Pauli repulsion energy; this is the main reason why the equilibrium metal/surface distance is decreased from 2.3 to 1.8 Å, which is the source of the double frustration effect [35]. (ii) A chemical bond is formed between the two electrons in the cavity and the metal orbitals [19,23]. As it will be explained in more detail in the following, this chemical bond is stronger than in the case of the regular surface, because the two delocalized electrons are more polarizable and can better overlap with the metal orbitals. (iii) Since the metal can get closer to the surface, it is subjected to a stronger electric field and thus the polarization contribution of the metal valence electrons is enhanced.

We now analyze how these three components of the metal/surface interaction change when the gold atom is absorbed on one of the neighboring sites of the defect (as usual, we limit our discussion to the first neighbor magnesium and the first neighbor oxygen). First of all, we remark that on these sites the interaction energy is stronger than in the case of the regular surface, being 1.62 eV on Magnesium and 1.19 eV on oxygen.

(i) The Pauli repulsion decreases only on top of the defect site. As a consequence, for example, the equilibrium height of the metal atom above the magnesium next to the defect does not change dramatically with respect to the regular surface. The decrease of Pauli repulsion

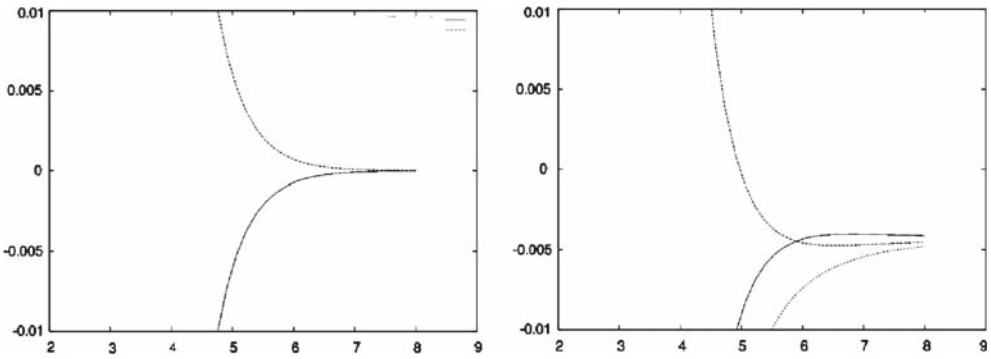

Fig. 3 Behavior of the electrostatic potential (in a.u.) along a direction perpendicular to the (100) terrace and on-top of the most characteristic sites of absorption on the surface. *Right* electrostatic potential on-top of the magnesium (*dashed line*) and oxygen (*continuos line*) sites of the regular surface. *Left* electrostatic potential on top of the vacancy (*dotted line*), of the magnesium first-neighbor (*dashed line*) and of the oxygen first-neighbor (*continuous line*) of the defect. Distances in a.u.

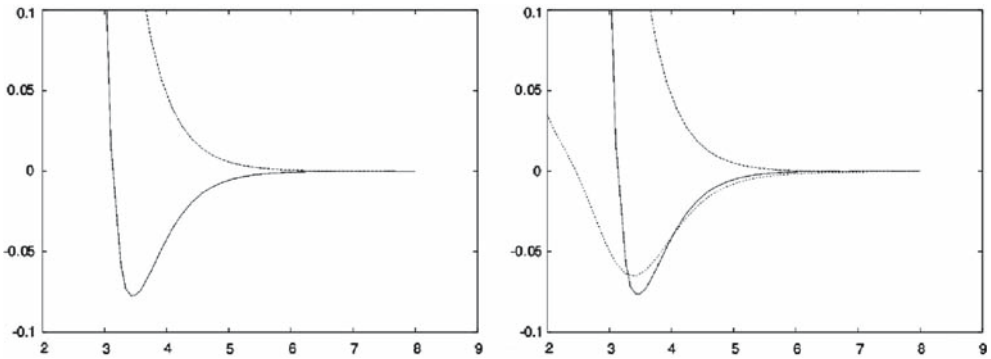

Fig. 4 Behavior of the electric field (in a.u.) along a direction perpendicular to the (100) terrace and on-top of the most characteristic sites of absorption on the regular and F_s-defected surface. *Right* electric field on-top of the magnesium (*dashed line*) and oxygen (*continuous line*) sites of the regular surface. *Left* electric field on top of the vacancy (*dotted line*), of the magnesium first-neighbor (*dashed line*) and of the oxygen first-neighbor (*continuous line*) of the defect. Distances in a.u.

thus does not account for the enhancement of the interaction energy.

(ii) The outward protrusion of the electron pair trapped in the vacancy generates an electrostatic potential in the neighborhood of the defect which is negatively shifted with respect to the regular surface. When a metal atom then approaches the surface, its valence electronic density is repelled far from the surface and a dipole, with its positive end pointing towards the surface, is formed. The interaction energy of such a dipole is thus enhanced by the negative shift of the electrostatic potential.

(iii) To analyze the polarization contribution, we show in Fig. 4 the electric field of the regular and defected surfaces. Somehow surprisingly, in spite of the overall negative shift of the potential, the behavior of the electric field appears to be very similar in the region relevant to metal absorption. The change in the polarization contribution is thus predicted to be of secondary importance in comparison to the stability enhancement due to the electrostatic potential — point (ii) — and to the chemical interaction — point (iv).

(iv) The chemical bonding contribution also plays an important role in explaining the observed behaviors.

To clarify this last point, it is useful to analyze the spin densities, reported in Fig. 5, that correspond to absorption of a single gold atom on the most significant sites of the regular and defective surface. In the first row of Fig. 5 we consider the absorption of the metal atom on the oxygen (left) and magnesium (right) sites of the regular surface. When gold interacts with the oxygen ion of the surface, a donation of electronic charge takes place from the surface to the partially depleted metal orbitals. For this reason, the spin density presents a *p*-character (centered on the surface oxygen) and a hybrid *s/d*-character (centered on the gold atom). On the contrary, when the gold atom is absorbed on the magnesium site, no chemical interaction occurs and the spin density is only

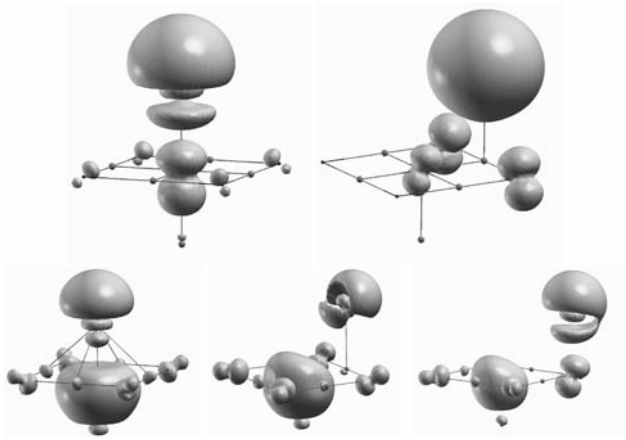

Fig. 5 Spin density isosurfaces of value −0.002 a.u. corresponding to the absorption of a gold atom on the most characteristic sites of the regular and of the F_s-defected surface. *First row* absorption on-top of the oxygen (*left*) and magnesium (*right*) sites of the regular surface. *Second row* absorption on-top of the vacancy (*left*), of the magnesium first-neighbor (*center*) and of the oxygen first-neighbor (*right*) of the defect

localized on the gold atom, where it approximately keeps the spherical shape of the unpaired valence s electron, as in the gas-phase.

The situation is remarkably different for the interaction with the F_s defect (second row of Fig. 5): in the case of absorption on-top of the vacancy (left), the strong interaction with the two electrons of the cavity is demonstrated by the fact that the spin density is concentrated both on the charge distribution in the cavity and on the metal atom. Analogously to what happens on the regular surface, a charge transfer takes place from the surface to the metal orbitals. With regard to the absorption on the magnesium site first-neighbor of the defect (center image), it is interesting to note that, differently from the regular surface, a noticeable chemical interaction still survives. As underlined above for the direct interaction with the defect, the possibility of forming stronger bonds is due to the delocalization of the two electrons of the vacancy. Furthermore, the chemical interaction survives, although a bit weaker, for the absorption of the gold atom on the oxygen first-neighbor of the defect. This chemical bonding contribution is substantially dependent only on the distance from the defect and the same is true for the negative shift of the electrostatic potential. This explains the *rotational invariance* observed for the metal/surface interaction [35].

In conclusion, we have shown that the presence of an F_s defect profoundly modifies the absorption features in the neighborhood of the defect. The surface Madelung potential is not sufficiently strong to confine within the vacancy the electron pair which protrudes out of the surface, thus: (a) decreasing the Pauli repulsion towards the electrons of absorbate species; (b) negatively shifting the electrostatic potential in a region around the defect extending up to 6–8 Å; (c) being able to form much stronger chemical bonds with incoming absorbates. This analysis rationalizes the double frustration and cylindrical invariance effect previously observed for the gold-oxide interaction. Finally, we stress that the results the results here reported are expected to hold not only in the case of gold-oxide interaction, but to be qualitatively true in general.

Acknowledgments GB and AF acknowledge financial support from the Italian CNR for the project SSA-TMN within the framework of the ESF EUROCORES SONS, and from the European Community Sixth Framework Project for the STREP Project GSOMEN (contract no. NMP-CT-2004-001594).

References

1. Osgood R (2006) Chem Rev 106:4379–4401
2. Barteau MA (1996) Chem Rev 96:1413–1430
3. Watanabe K, Menzel D, Nilius N, Freund HJ (2006) Chem Rev 106:4301–4320
4. Delmon B (2006) Catal Today 117:69–74
5. Lauritsen JV et al (2006) Nanotechnology 17:3436–3441
6. Schoiswohl J, Surnev S, Netzer FP (2005) Top Catal 36:91–105
7. Tada M, Iwasawa Y (2006) Chem Commun, pp. 2833–2844
8. Freund HJ (2002) Surf Sci 500:271–299
9. Barth C, Henry CR (2003) Phys Rev Lett 91:196102
10. Coluccia S, Baricco M, Marchese L, Martra G, Zecchina A (1993) Spectrochim Acta A 49:1289–1298
11. Mellor IM, Burrows A, Coluccia S, Hargreaves JSJ, Joyner RW, Kiely CJ, Martra G, Stockenhuber M, Tang WM (2005) J Catal 234:14–23
12. Sterrer M, Risse T, Freund HJ (2006) App Catal A 307:58–61
13. Sterrer M, Fischbach E, Heyde M, Nilius N, Rust HP, Risse T, Freund HJ (2006) J Phys Chem B 110:8665–8669
14. Barth C, Henry CR (2006) Nanotechnology 17:S155–S161
15. Barcaro G, Fortunelli A (2005) J Comp Theor Chem 1:972–985
16. Giordano L, Di Valentin C, Goniakowski J, Pacchioni G (2004) Phys Rev Lett 92:096105
17. Sterrer M, Yulikov M, Fischbach E, Heyde M, Rust HP, Pacchioni G, Risse T, Freund HJ (2006) Angew Chem Int Ed 45:2630–2632
18. Pacchioni G, Pescarmona P (1998) Surf Sci 412/413:657
19. Matveev AV, Neyman K, Yudanov I, Rösch N (1999) Surf Sci 426:123–139
20. Bogicevic A, Jennison DR (1999) Surf Sci 437:L741
21. Mori-Sanchez P, Recio JM, Silvi B, Sousa C, Martin Pendas A, Luana V, Illas F (2002) Phys Rev B 66:075103
22. Yang Z, Wu R, Zhang Q, Goodman DW (2002) Phys Rev B 65:155407
23. Del Vitto A, Pacchioni G, Delbecq F, Sautet P (2005) J Phys Chem B 109:8040
24. Yoon B, Häkkinen H, Landman U, Wörz AS, Antonietti JM, Abbet S, Judai K, Heiz U (2005) Science 307:403
25. Walter M, Häkkinen H (2005) Phys Rev B 72:205440
26. Neyman KM, Inntam C, Matveev AV, Nasluzov VA, Rosch N (2005) J Am Chem Soc 127:11652
27. Moseler M, Häkkinen H, Landman U (2002) Phys Rev Lett 89:176103
28. Pacchioni G (2003) Chem Phys Chem 4:1041
29. Sousa C, Illas F (2001) J Chem Phys 115:1435
30. Wendt S, Kim YD, Goodman DW (2003) Prog Surf Sci 74:141
31. Sanchez A, Abbet S, Heiz U, Schneider WD, Häkkinen H, Barnett RN, Landman U (1999) J Phys Chem A 103:9573–9578
32. Molina LM, Hammer B (2005) J Chem Phys 123:161104

33. Neyman K M, Inntam C, Moskaleva L V, Rösch N (2006) Chem Eur J 13:277
34. Yulikov M, Sterrer M, Heyde M, Rust HP, Risse T, Freund HJ, Pacchioni G, Scagnelli A (2006) Phys Rev Lett 96:146804
35. Barcaro G, Fortunelli A (2006) J Phys Chem B 110:21021–21027
36. Saunders VR, Dovesi R, Roetti C, Orlando R, Zicovich-Wilson CM, Harrison NM, Doll K, Civalleri B, Bush IJ, D'Arco P, Llunell M, CRYSTAL 2003 User Manual (2003) Turin University
37. Becke AD (1993) J Chem Phys 98:5648–5652
38. McCarthy MI, Harrison NM (1994) Phys Rev B 49:8574–8582
39. Dovesi R, Roetti C, Freyria-Fava C, Aprà E, Saunders VR, Harrison NM (1992) Philos Trans R Soc London Ser A 341:203
40. Kokalj A (1999) J Mol Graph Model 17:176
41. Sterrer M, Fischbach E, Risse T, Freund HJ (2005) Phys Rev Lett 94:186101